NeuroImage 102 (2014) 24–34

Contents lists available at ScienceDirect

NeuroImage

journal homepage: www.elsevier.com/locate/ynimg

Review

EEG–fMRI integration for the study of human brain function

João Jorge [a,b], Wietske van der Zwaag [b], Patrícia Figueiredo [a,*]

[a] Institute for Systems and Robotics, Department of Bioengineering, Instituto Superior Técnico, Technical University of Lisbon, Lisbon, Portugal
[b] Biomedical Imaging Research Center, École Polytechnique Fédérale de Lausanne, Lausanne, Switzerland

ARTICLE INFO

Article history:
Accepted 25 May 2013
Available online 31 May 2013

Keywords:
EEG–fMRI
Multimodal fusion
Brain function

ABSTRACT

Electroencephalography (EEG) and functional magnetic resonance imaging (fMRI) have proved to be extremely valuable tools for the non-invasive study of human brain function. Moreover, due to a notable degree of complementarity between the two modalities, the combination of EEG and fMRI data has been actively sought in the last two decades. Although initially focused on epilepsy, EEG–fMRI applications were rapidly extended to the study of healthy brain function, yielding new insights into its underlying mechanisms and pathways. Nevertheless, EEG and fMRI have markedly different spatial and temporal resolutions, and probe neuronal activity through distinct biophysical processes, many aspects of which are still poorly understood. The remarkable conceptual and methodological challenges associated with EEG–fMRI integration have motivated the development of a wide range of analysis approaches over the years, each relying on more or less restrictive assumptions, and aiming to shed further light on the mechanisms of brain function along with those of the EEG–fMRI coupling itself. Here, we present a review of the most relevant EEG–fMRI integration approaches yet proposed for the study of brain function, supported by a general overview of our current understanding of the biophysical mechanisms coupling the signals obtained from the two modalities.

Contents

Introduction

Scalp electroencephalography (EEG) has been used to study brain function for almost a century. Its sub-millisecond temporal resolution allows for adequate sampling of the rich temporal dynamics of neuronal population activity, as expressed by electric potential fluctuations

* Corresponding author at: Institute for Systems and Robotics, Department of Bioengineering, Instituto Superior Técnico, Technical University of Lisbon, Av. Rovisco Pais, 1, 1049-001 Lisboa, Portugal. Fax: +351 218418291.
E-mail address: patricia.figueiredo@ist.utl.pt (P. Figueiredo).

1053-8119/$ – see front matter © 2013 Elsevier Inc. All rights reserved.
http://dx.doi.org/10.1016/j.neuroimage.2013.05.114

propagated to the scalp. However, sensitivity is biased by cell type and architecture (Nunez and Silberstein, 2000). Moreover, acquisitions typically involve only up to a few hundred electrodes positioned on the scalp, which together with volume conduction through the head, particularly the skull, results in a poor spatial resolution and signal-to-noise-ratio (SNR). Such limitations make EEG source reconstruction a notably ill-posed problem (Michel et al., 2004). In contrast, blood oxygenation level-dependent (BOLD) functional magnetic resonance imaging (fMRI) (Ogawa et al., 1990) allows versatile trade-offs between SNR, spatiotemporal resolution and field-of-view. BOLD acquisitions can achieve sub-millimeter spatial resolution, resulting in a tremendous functional localization power (Yacoub et al., 2007). However, temporal resolution is limited to a few hundred milliseconds or even seconds. Furthermore, the BOLD contrast does not directly reflect neuronal activity, but rather a complex and still poorly understood combination of hemodynamic and metabolic effects, with inherently slower dynamics (Logothetis, 2008).

Due to the remarkable complementarity between the two techniques, EEG–fMRI has become a highly desirable multimodal approach (Babiloni et al., 2004). The first EEG recordings performed inside an MR scanner were accomplished shortly after fMRI started being applied to humans (Ives et al., 1993), and aimed for a better spatial localization of epileptic networks in patients undergoing presurgical evaluation (Patel et al., 1999). Due to their strong static magnetic field and rapidly-varying gradients during image acquisition, MR scanners impose a harsh environment for EEG recording, raising important issues regarding both data quality and patient safety (Lemieux et al., 1997). This encouraged a remarkable course of technological advancements in EEG system design and acquisition protocols (Allen et al., 1998; Goldman et al., 2000; HuangHellinger et al., 1995; Krakow et al., 1999). Improvements in sampling synchronization led to an effective reduction of gradient-induced EEG artifacts (Allen et al., 2000; Mandelkow et al., 2006), allowing for the transition from interleaved (Bonmassar et al., 1999; Kruggel et al., 2000) to truly simultaneous acquisitions, which are now widely used both in clinical (Lemieux et al., 2001) and non-clinical contexts (Goldman et al., 2002; Moosmann et al., 2003). Nevertheless, interleaved approaches do provide cleaner data with less complex hardware setups, and are still frequently used (Eichele et al., 2005). Considerable work has also been dedicated to important MR-induced EEG artifacts related to the cardiac cycle (Allen et al., 1998; Bonmassar et al., 2002; Debener et al., 2008; Mullinger et al., 2013) and to certain scanner components, such as the Helium compression pumps (Mullinger et al., 2008a) and patient ventilation systems (Nierhaus et al., 2013). In parallel, some attention has also been devoted to MR image artifacts created by the presence of EEG materials (Mullinger et al., 2008b; Vasios et al., 2006).

Despite having its origins in the study of epileptic networks, EEG–fMRI applications were rapidly extended to the study of healthy human brain function (Debener et al., 2006; Herrmann and Debener, 2008). Nevertheless, combined studies involve several conceptual and methodological challenges at the level of experimental design and data acquisition, modality-specific data processing and multimodal data integration. Here, we review some of the most relevant EEG–fMRI data integration approaches proposed to date, following a brief overview of the current understanding of the biophysical mechanisms linking EEG and fMRI signals to the underlying neuronal activity. We leave aside the more technical questions associated with acquisition, artifact reduction and safety, which have been covered elsewhere (Laufs, 2012; Lemieux et al., 1997; Mullinger and Bowtell, 2011).

Neurophysiological bases of EEG and BOLD

EEG signals

Although surface EEG is often regarded as a direct measure of neuronal activity, a complete understanding of its underlying neurophysiological correlates has in fact not yet been achieved. Neuronal activity is mediated by synaptic interactions and action potential propagation (spiking). In each neuron, synaptic inputs tend to induce transmembranous ionic currents (postsynaptic activity) that give rise to intra and extracellular currents along the membrane (Niedermeyer and Lopes da Silva, 2005). The latter generate the so-called local field potentials (LFPs) and can be seen as equivalent electric dipoles between the stimulated dendrites and sub-synaptic regions. For favorable cell geometries and arrangements, the electric field resulting from the summation of such dipolar potentials can be picked up by electrodes on the scalp (Dale and Halgren, 2001). However, this also implies an intrinsic bias towards the activity of cortical pyramidal cells, which are mostly oriented perpendicularly to the cortical surface, as opposed to other cell types such as interneurons. Membrane potential oscillations and after-potentials following spike propagation share the frequency domain of postsynaptic activity (altogether termed perisynaptic activity), and will also contribute to LFPs (Logothetis, 2008). While action potentials also induce currents along the membrane (locally measurable as multi-unit activity, MUA), evidence suggests that the faster nature of these phenomena prevents a favorable summation of large population activity (Nunez and Silberstein, 2000). Nevertheless, recent studies have shown that features from certain scalp EEG frequency bands can be used to infer spiking activity as well (Whittingstall and Logothetis, 2009). Likewise, glial cells can give rise to ionic flows when locally depolarized, which can also contribute to LFPs (Niedermeyer and Lopes da Silva, 2005).

EEG signals typically contain rich temporal profiles, which include transient responses specific to the applied stimuli (termed event-related potentials, ERPs), and a time-varying composition of frequencies commonly referred to as brain rhythms. These rhythms can be attributed to regional synchronous oscillatory activity, but their underlying mechanisms depend strongly on the frequency range considered (Jefferys et al., 2012; Niedermeyer and Lopes da Silva, 2005). Frequency band-specific fluctuations may arise in correlation with external stimuli, as the so-called event-related synchronization (ERS) or desynchronization (ERD) (Pfurtscheller and Lopes da Silva, 1999).

The BOLD contrast

The BOLD signal is a T_2^* (and also T_2) based contrast that is sensitive to the local concentration of deoxyhemoglobin (dHb). In contrast with oxyhemoglobin and brain tissues in general, dHb is a paramagnetic substance, and hence produces field distortions across the capillaries that accelerate local transverse spin relaxation leading to signal loss in $T_2(^*)$-weighted images (Ogawa et al., 1990). In the brain, dHb fluctuations can be expressed as a combination of changes in cerebral blood flow (CBF), cerebral blood volume (CBV), and the cerebral metabolic rate of O_2 ($CMRO_2$) (Buxton et al., 1998; Davis et al., 1998). Neuronal activity is tightly linked to the metabolic pathways of ATP production, which drive $CMRO_2$ fluctuations, but is also known to exert a more direct influence on local CBF (Attwell et al., 2010; Logothetis, 2002). Overall, a local increase in neuronal activity will not only raise $CMRO_2$ but also typically induce a strong increase in CBF, mediated by local autoregulation mechanisms, resulting in a net decrease in dHb concentration, and hence a positive BOLD response (Jezzard et al., 2001). This is a rather slow phenomenon, with a delay of several seconds from the activity onset and a slow decay after return to baseline.

Due to this indirect coupling, BOLD fluctuations must be carefully interpreted (Logothetis, 2008). For instance, while deactivated populations may express negative BOLD responses (Shmuel et al., 2006), complex arrangements of competing excitatory and inhibitory activity can have unpredictable outcomes (Lauritzen and Gold, 2003). Neurovascular coupling has been found to vary across brain regions (de Munck et al., 2007; Goense et al., 2012), and modifications have also been identified in certain pathological conditions such as epilepsy (Grouiller et al., 2010), cortical spreading depression, brain ischemia and Alzheimer's disease (Attwell et al., 2010). Similarly, much

work has been devoted to understanding which aspects of neuronal activity are best reflected in BOLD fluctuations. Although not undisputedly (Mukamel et al., 2005), evidence suggests that LFPs are more tightly correlated with BOLD than MUA (Logothetis, 2002; Rauch et al., 2008). While this points to perisynaptic activity as the best correlate of BOLD fluctuations, the problem becomes even more complex as different LFP frequency bands tend to show distinct, context-dependent correlations with BOLD (Niessing et al., 2005; Whitman et al., 2013). Finally, besides neurons, other cell types such as astrocytes can influence hemodynamic fluctuations significantly (Schummers et al., 2008). Moreover, ongoing physiological processes such as the cardiac and respiratory cycles can also introduce important confounds (Jorge et al., 2013; Kruger et al., 2001).

Substrates of EEG, fMRI and behavior

While strongly dependent on the underlying neuronal activity, the signals captured by either EEG or fMRI form a complex, biased expression of only part of that activity. As illustrated in Fig. 1, their neuronal substrates can be schematized as two partially-overlapping domains contained inside the larger pool of neuronal activity (Rosa et al., 2010a), which can itself be divided into an event-related domain, comprising evoked activity associated to an experimental paradigm, and an event-unrelated domain, comprising spontaneous activity (Debener et al., 2006). Behavior can also be considered as a third domain of observation (Laufs, 2012). These representations highlight the subtleties of multimodal integration—for example, a behavioral change may be accompanied by measurable changes in EEG, fMRI, or both, but the underlying sources may differ (Nunez and Silberstein, 2000). Likewise, different integration approaches involve different assumptions regarding this issue, and thus carry specific vulnerabilities when applied to the complex dynamics of brain function (Daunizeau et al., 2005; Im et al., 2005; Laufs et al., 2006; Martinez et al., 1999; Regenbogen et al., 2012).

EEG–fMRI integration

Here, we review the different approaches proposed for EEG–fMRI integration, at the level of experimental design, modality-specific data processing, and especially multimodal data analysis. In the latter, the reviewed studies were grouped into comparison, asymmetrical and symmetrical integration approaches, as schematized in Fig. 2.

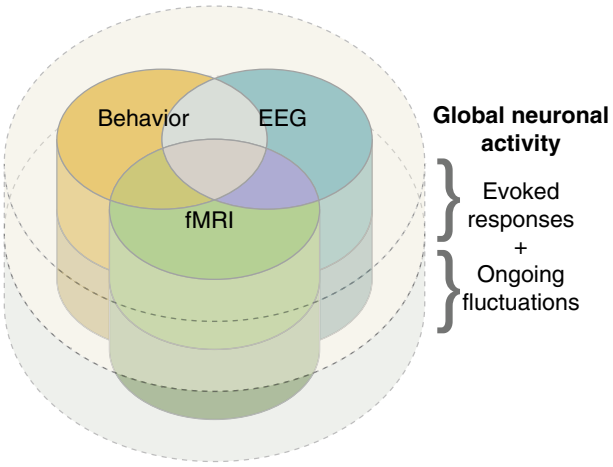

Fig. 1. EEG, fMRI and behavior can be seen as separate measures of distinct, only partially overlapping substrates of the whole domain of brain activity. This larger domain can be divided into externally-evoked activity, associated to an experimental protocol, and spontaneous activity, comprising ongoing fluctuations.

Experimental design

A fundamental question regarding data acquisition is whether EEG and fMRI should be acquired separately (in different sessions with similar experimental paradigms) or simultaneously. More specifically, this relates to whether the scientific question at hand can be answered satisfactorily from separately-acquired data (Debener et al., 2006). Separate acquisitions carry two main advantages. First, due to the different temporal scales of electrophysiology and hemodynamics, most event-related designs cannot be optimized for both modalities simultaneously. For example, while the maximum-amplitude responses to alternating visual checkerboards have been identified at a reversing frequency of 8 Hz for both EEG and fMRI (Singh et al., 2003; Wan et al., 2006), the full duration of typical EEG visually-evoked potentials (VEPs) cannot be resolved at such a high frequency (Singh et al., 2003). Additionally, in interleaved acquisitions, the inclusion of "MR-silent" periods affects the choice of repetition time (TR) and may further constrain stimulation timings (Garreffa et al., 2004). A second and often more important advantage is that separate acquisitions are not susceptible to the specific artifacts of simultaneous EEG–fMRI.

Nevertheless, certain experimental confounds and applicability limitations can only be overcome with simultaneous protocols. The distinct environments in which EEG and fMRI are typically acquired can present very different and potentially confounding spurious stimuli (Novitski et al., 2003; Sammer et al., 2005). Separate sessions can also introduce training or habituation effects (Debener et al., 2002), along with different subjective impressions and experiences, as well as emotional and motivational states (Boly et al., 2007; Busch et al., 2009; Raichle and Gusnard, 2005). Regarding applicability, the study of spontaneous activity, such as in resting-state experiments (Mantini et al., 2007; Scheeringa et al., 2008), simply cannot be accomplished in separate sessions. The same applies to the study of trial-by-trial fluctuations, which have been found to predict additional variability across modalities (Becker et al., 2011; Debener et al., 2005).

Considering the distinct timescales of EEG and fMRI responses, experimental paradigms must be carefully designed to highlight the phenomena of interest in each modality (Garreffa et al., 2004), while dealing with potential sensitivity and specificity compromises (Liu et al., 2001). Along this line, parametric designs, where stimuli are presented with controlled variations of a specific parameter, have proved to be particularly insightful (Horovitz et al., 2004; Liu et al., 2010; Mulert et al., 2005; Schicke et al., 2006).

Generic data processing

Before integrated analysis, both EEG and fMRI data are usually subjected to a number of modality-specific preprocessing stages (Fig. 2). For fMRI, typical steps include image reconstruction from sampled K-space data, motion and slice-timing correction, spatial smoothing and normalization, and slow-drift removal (Smith et al., 2004; Strother, 2006). On the EEG side, common steps are slow-drift removal, epoch extraction, electrode re-referencing and data re-sampling (Delorme and Makeig, 2004). For data acquired simultaneously with fMRI, additional steps must be incorporated to reduce gradient and pulse artifacts, usually through average template subtraction (Allen et al., 1998, 2000), possibly complemented with principal component analysis (PCA)-based techniques (Niazy et al., 2005). Different algorithms provide varying, often frequency-specific balances between noise reduction and signal preservation (Freyer et al., 2009; Grouiller et al., 2007).

A few other techniques are worthy of mention given their frequent use in EEG–fMRI studies. For instance, frequency-specific EEG power fluctuations, particularly in the alpha (typically 8–12 Hz) and gamma (25–100 Hz) bands, have been extensively analyzed. Such information is associated with a time–frequency representation or "spectrogram", which can be obtained by segmenting the EEG

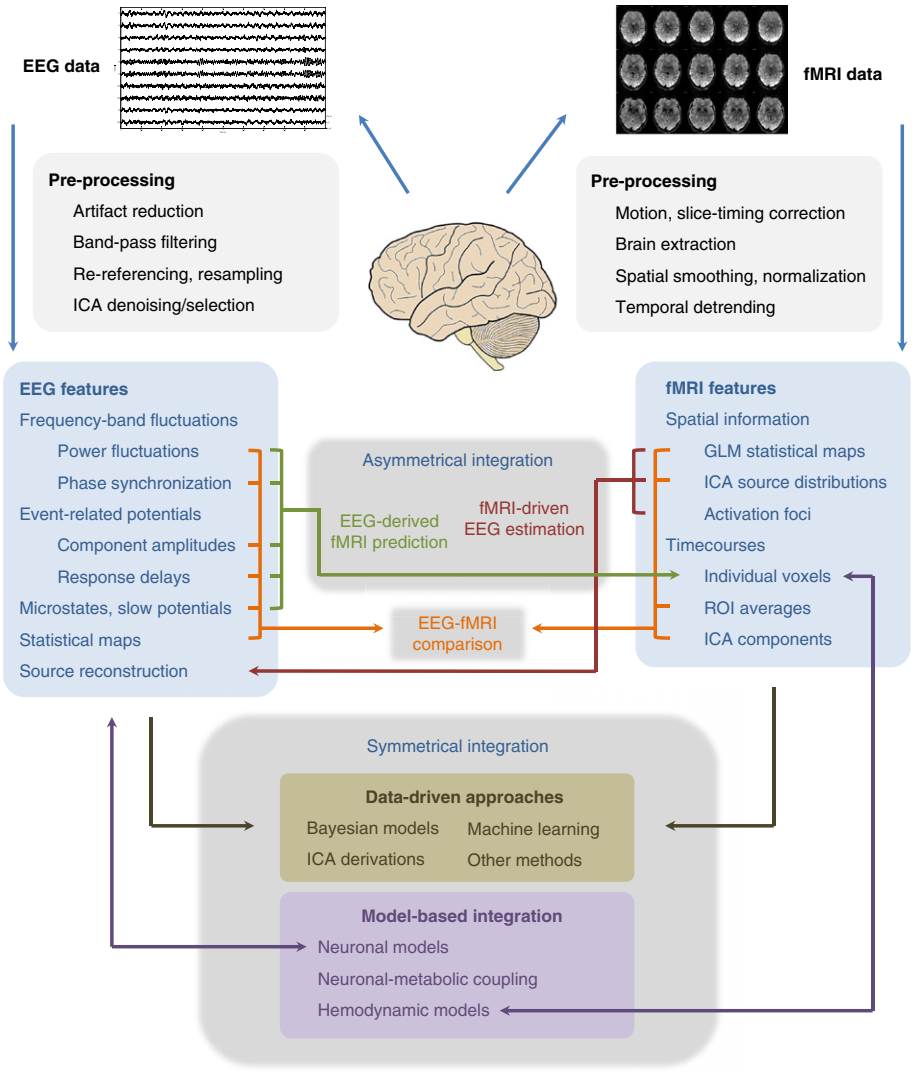

Fig. 2. A general scheme of the main EEG–fMRI data integration approaches proposed in the literature, including purely comparative, asymmetrical and symmetrical techniques.

timecourses into small epochs and Fourier-transforming each epoch separately (Goldman et al., 2002). This approach can be further improved with multi-tapering methods (Thomson, 1982), which minimize the variance of higher-frequency estimates (Martuzzi et al., 2009; Scheeringa et al., 2011). Also, instead of Fourier transforms, some authors have opted for wavelet-based analysis (Mizuhara et al., 2005; Moosmann et al., 2003; Mulert et al., 2010), which allows a versatile tradeoff between time and frequency resolutions (Tallon-Baudry et al., 1998).

As for fMRI, the identification of brain regions displaying significant signal changes in association with an external stimulus or task is often performed by general linear model (GLM) analysis. Here, a model of the activity of interest is convolved with a suitable hemodynamic response function (HRF) and used for voxel-by-voxel regression analysis, yielding statistical maps of associated BOLD changes (Worsley and Friston, 1995). The adopted HRF represents the transfer function assumed to link neuronal activity to the BOLD signal, and can be designed based on an empirically-derived "canonical form" (Friston et al., 1998) or specifically adapted to the data and context at hand (de Munck et al., 2007; Grouiller et al., 2010; Logothetis et al., 2001).

Finally, in both modalities alike, a growing number of studies have incorporated the use of independent component analysis (ICA), which aims to decompose the data into a set of statistically-independent sources (Bridwell et al., 2012; Eichele et al., 2008; Marques et al., 2009; Masterton et al., 2013). Both for EEG (Brown et al., 2001) and fMRI (McKeown and Sejnowski, 1998), ICA typically generates a set of timecourses associated to particular spatial distributions in the brain or on the scalp. These sources can then be selected or excluded from further analysis steps based on their spatial or temporal patterns (Scheeringa et al., 2008). Given the different nature of the data from each modality, temporal ICA is usually applied to EEG data, while spatial ICA is a more common choice for fMRI (Calhoun et al., 2009).

Data integration: comparison approaches

Many EEG–fMRI studies investigating neurovascular coupling have employed purely comparative approaches, analyzing which measures of each modality yield the most significant correlations between the two (Fig. 2). For instance, seminal studies involved the implantation of cortical microelectrodes in experimental animals, allowing for the direct comparison of LFP and MUA measures with the local BOLD response. Logothetis et al. (2001) performed occipital microelectrode recordings simultaneously with fMRI in monkeys, during visual stimulation. LFP and MUA fluctuations were estimated from lower and higher frequency bands, respectively, convolved with data-derived HRFs, and compared to local BOLD responses. Niessing et al. (2005) further

separated LFP information into different frequency bands, and correlated their power distributions with trial-by-trial fluctuations in the hemodynamic response.

More recently, a few groups have compared fMRI with intracranial EEG (icEEG, or "electrocorticography", ECoG) recordings, in patients undergoing presurgical evaluation. In one of the few simultaneous studies published so far, Carmichael et al. (2011) acquired icEEG–fMRI during a finger-tapping task. Here, icEEG signals were converted to a time–frequency representation, HRF-convolved, and correlated with the average BOLD timecourse in the task-activated region, allowing for a direct frequency- and location-specific comparison. Two other reports on simultaneous icEEG–fMRI have focused on the study of interictal epileptiform activity, analyzing the propagation dynamics and hemodynamic correlates of occurring discharges (Cunningham et al., 2012; Vulliemoz et al., 2011). Separate recordings have also been explored in certain cognitive studies (Lachaux et al., 2007). For example, Harvey et al. (2013) acquired separate fMRI and icEEG data from occipital and parietal areas, while visually stimulating distinct neuronal populations with drifting checkerboard bars of varying orientation. BOLD responses were used to identify the aggregate receptive fields associated with each stimulus, and icEEG signals yielded frequency-specific power timecourses for each field and its surrounding areas. This evinced how different frequency bands are involved in local activation and surround suppression mechanisms in the primary visual cortex. Although limited in brain coverage and applicability, the higher specificity and SNR of intracranial recordings are sparking a rapidly-growing interest in their integration with fMRI (Hermes et al., 2012).

Whole-brain approaches integrating scalp EEG and fMRI have also proven to be powerful tools for comparative analysis. For example, Martuzzi et al. (2009) acquired separate scalp EEG and fMRI data during visual stimulation. EEG data from the pre- and post-stimulus onset periods of each trial were used for source reconstruction (Michel et al., 2004), and Fourier-transformed. By comparing these two periods across trials, it was possible to determine frequency-specific statistical maps of task-related power variation, which could then be directly compared with the corresponding task-related BOLD maps, highlighting region- and frequency-specific couplings. In a similar approach, Yuan et al. (2010) investigated the relationship between task-related changes in alpha and beta power and the BOLD response during motor imagery and movement. In another example, targeting the dynamics of speech and language lateralization, Morillon et al. (2010) computed average BOLD timecourses for a series of atlas-based regions, including language networks, and compared them to frequency-specific, HRF-convolved power timecourses extracted from a fronto-central electrode.

Important work has also been dedicated to the study of resting-state networks (RSNs), consisting of spontaneous but spatially-correlated fluctuations in brain activity (Biswal et al., 1995; Fox and Raichle, 2007). Mantini et al. (2007) acquired simultaneous EEG–fMRI data from awake, resting subjects. Five EEG power timecourses were computed from sub-bands of interest, and spatial ICA was applied to the fMRI data in order to identify a set of consistent RSNs. The RSN timecourses were then correlated to each of the frequency-specific power timecourses, to assess whether each RSN could be linked to a specific spectral power profile. In a latter work, Meyer et al. (2013) studied the temporal stability of these spectral profiles.

Data integration: asymmetrical approaches

In general, asymmetrical integration approaches rely on information extracted from one of the two modalities to drive or constrain the analysis of the other (Fig. 2), aiming to complement its specific spatiotemporal limitations and yield better estimates and predictions. This idea has motivated a wide variety of methods (Herrmann and Debener, 2008), which can be grouped into two main categories: fMRI-driven EEG estimation, and EEG-derived BOLD prediction. In both cases, results must be interpreted carefully, as these approaches tend to rely heavily on the assumption that the neuronal substrates of EEG and fMRI are essentially coincident.

fMRI-driven EEG estimation

Powerful integration methods have been proposed where statistical maps of paradigm-related BOLD signal changes are used to guide or constrain EEG source reconstruction. Volume conduction through the head and the limited spatial sampling of scalp EEG, along with other limitations (Nunez and Silberstein, 2000), make the reconstruction problem markedly ill-posed and depth-dependent, requiring the incorporation of spatial constraints and regularization terms (Michel et al., 2004). High-spatial resolution techniques such as MRI can provide useful complementary information for this task, namely in the design of highly-detailed, subject-specific head volume conductance maps (Dale and Sereno, 1993; Katscher et al., 2009; Lemieux et al., 1996; Wolters et al., 2006). Similarly, functional information given by fMRI and PET has been found useful to provide spatial constraints and better-informed regularization criteria (Heinze et al., 1994).

Many studies rely on reconstruction algorithms that model the neuronal generators of EEG potentials as a predetermined number of electrical dipoles with fixed positions, spread across the cortical surface (Dale and Sereno, 1993). Here, functional information from fMRI can be used to guide the selection of dipole numbers and positions (Ullsperger and von Cramon, 2001). For example, Bledowski et al. (2004) acquired EEG and fMRI data from subjects undergoing a visual oddball paradigm, in order to investigate the contribution of different stationary brain sources to the elicited ERPs. Dipole "seeds" were positioned at the foci of clusters exhibiting significant, oddball-specific BOLD responses, and inverse solutions were then obtained for the trial-averaged ERPs elicited by each stimulus condition, along with "differential ERPs" comparing standard to oddball categories. Brass et al. (2005) and Meyer et al. (2012) used similar approaches to study the interaction between different cortical structures during specific cognitive processes. Additionally, EEG inverse solutions can be further conditioned by specifying not only dipole positions but also their orientations (Menon et al., 1997; Vanni et al., 2004). Although undeniably valuable, BOLD-derived dipole seeding approaches contain important limitations. Due to the low spatial resolution of EEG, dipole sources placed too close to each other are susceptible to "cross-talking" effects, leading to erroneous timecourse reconstructions (Vanni et al., 2004). In addition, the existence of fMRI-blind EEG sources can never be completely ruled out, and, when present, these sources may act as important confounds.

Alternative approaches have been proposed where fMRI is used not to specify source locations but, instead, to guide the optimization of distributed source models, through the inclusion of a priori information in the cost-function terms. Using a predetermined cortical surface distribution of dipole sources, Dale et al. (2000) adopted a Bayesian formulation for the problem of determining the pattern of activity that is most consistent with a given set of EEG and fMRI observations, and used task-related BOLD statistical maps to model the spatial covariance of source dipole strength. This yielded significant improvements in spatial resolution, as compared to non-informed inverse solutions. In an analogous approach, Babiloni et al. (2004) introduced fMRI information through a nonlinear function of the BOLD statistical maps, which included a free parameter to tune the strength of the introduced bias. In a subsequent study addressing functional cortical connectivity, the authors applied this technique to estimate high-temporal resolution source waveforms in specific regions-of-interest, and then applied directed transfer function techniques to investigate the directions of information flow between regions (Babiloni et al., 2005). Ahlfors and Simpson (2004) presented an alternative formulation based on concepts of subspace regularization, where the inverse solution minimizes the distance to a subspace defined by the fMRI estimates. Daunizeau et al. (2005) proposed to characterize the relevance of fMRI-derived spatial priors in a Bayesian

framework, by means of a quantitative comparison with non-informative priors.

Other authors built upon these ideas to achieve increasingly more reliable reconstructions (Liu and He, 2008; Ou et al., 2010). For example, aiming for a more accurate description of the neurovascular coupling implicit in fMRI-guided reconstructions, Liu and He (2008) proposed to link fMRI activation specifically to the time integral of local source power during ERP generation. Applied to the study of ERPs elicited in bilateral visual integration, these modifications yielded more focal activations with higher spatial resolution, while preserving a general agreement with purely EEG-based inverse solutions (Liu et al., 2009).

EEG-derived BOLD prediction

In a somewhat reciprocal approach to fMRI-driven EEG estimation, numerous studies have opted for the extraction of activity timecourses from EEG data and used them to model certain components of BOLD signal variance ("integration by prediction"). In the vast majority of studies, EEG-derived timecourses are HRF-convolved, down-sampled to match fMRI acquisition timings, and then used as regressors in voxel-wise GLM analyses. While these stages are relatively common, the selection of relevant EEG features can itself rely on very diverse assumptions and hypotheses regarding the EEG–BOLD coupling, and various approaches have been proposed.

Frequency band-specific power fluctuations are possibly the most extensively analyzed EEG feature for fMRI prediction. In an early example, Goldman et al. (2002) investigated the BOLD correlates of alpha fluctuations in a resting-state simultaneous EEG–fMRI study. An alpha-band power timecourse was extracted from occipital electrodes, HRF-convolved and voxel-wise correlated with BOLD data, showing regions with significant correlation or anti-correlation with the alpha rhythm. Several authors have investigated the robustness of this approach, assessing artifact sensitivity (Laufs et al., 2003), inter-subject and inter-session variability (Goncalves et al., 2006), and physiological confounds (de Munck et al., 2008). Likewise, by including multiple power timecourses extracted from different frequency bands, a number of studies have shown the importance of multiple-band interactions for a more complete representation of BOLD activity (de Munck et al., 2009; Giraud et al., 2007; Scheeringa et al., 2011; Scholvinck et al., 2010).

Although meaningful correlations between BOLD and EEG power timecourses have often been reported (Laufs et al., 2006; Moosmann et al., 2003; Scheeringa et al., 2008), these carry strong assumptions regarding the EEG–BOLD coupling, and must be considered carefully. Supporting the approach, it has been suggested that, while both neuronal and hemodynamic responses behave in a highly nonlinear manner with stimulus strength and duration (Logothetis, 2002), the relationship between EEG source power and BOLD amplitude remains itself close to linear, both in positive (Liu et al., 2010; Wan et al., 2006) and negative responses (Arthurs et al., 2007). Nonetheless, recent studies investigating diverse transfer functions between EEG and BOLD fluctuations have identified particularly informative new metrics (Leite et al., 2013; Rosa et al., 2010b). Notably, the EEG "root-mean-squared frequency", based on a heuristic proposed by Kilner et al. (2005), was found to be superior to power-weighted metrics for BOLD prediction, highlighting the importance of relative power redistribution across the spectrum, over absolute power fluctuations.

Besides power-related fluctuations, frequency-specific phase synchronization has also been identified as a meaningful EEG feature. Mizuhara et al. (2005) studied the dynamics of long-range EEG phase synchronization during an arithmetic task. Wavelet analysis was used to estimate instantaneous phase timecourses at each frequency bin and channel, and a phase synchronization index (PSI) was then computed for each channel pair, frequency bin and data epoch. Channel pairs and frequencies associated with significant, task-dependent PSI modulation were identified, and the respective PSI timecourses were HRF-convolved and used for GLM analysis. Another approach, adopted by Jann et al. (2009) and Kottlow et al. (2012), focused on the dynamics of global field synchronization (GFS). Here, EEG data were epoched and Fourier-transformed, and for each epoch and frequency bin, the sine and cosine values of each channel were plotted as a point in a 2D diagram. The shape of this point cloud would then indicate the amount of phase synchronization across all channels, quantified by PCA to yield a single GFS value (per frequency bin, per epoch).

Event-related studies also often elicit trial-specific ERPs with potentially informative dynamics. In a parametric approach, Eichele et al. (2005) studied an auditory target detection task where target predictability was systematically manipulated. The single-trial amplitudes of three ERP "frames" were found exceptionally effective for predicting BOLD fluctuations in certain regions, independently from the common auditory response. In a later study, Benar et al. (2007) further identified EEG response latency as an additional feature with relevant BOLD predictive power. In a visual discrimination task, Philiastides and Sajda (2007) designed regressors to model three response components varying independently with task type and difficulty, as identified from EEG responses analyzed in previous experiments (Philiastides and Sajda, 2006). These regressors were then used to find brain regions potentially involved in the generation of each component. Other authors have instead focused on spontaneous trial-by-trial fluctuations (Debener et al., 2005; Novitskiy et al., 2011). In a recent example, Jaspers-Fayer et al. (2012) investigated the neuronal sources involved in the processing of emotional auditory stimuli by analyzing an early EEG component elicited specifically by emotional stimulation. Single-trial EEG amplitudes were extracted from early time windows associated with this component, orthogonalized with respect to standard task-related effects, and used as GLM regressors. Other studies have explored the predictive capabilities of slow cortical potentials (Hinterberger et al., 2005; Khader et al., 2008; Nagai et al., 2004).

A crucial aspect of EEG feature extraction is the approach used to isolate the patterns of interest from the remaining information and artifacts, which strongly depends on their SNR and specificity. For example, alpha activity can reach high amplitudes in occipital regions, allowing for good-quality estimates simply by selecting a few posterior electrodes (Laufs et al., 2006; Mo et al., 2013). In other applications, more powerful approaches are often required. ICA-based techniques are particularly useful, as the resulting patterns can be easily discriminated according to their spatial, temporal, and spectral profiles (Becker et al., 2011; Feige et al., 2005; Formaggio et al., 2011). Event-related studies also often include additional feature extraction steps, such as selective epoching and averaging (Kottlow et al., 2012; Scheeringa et al., 2011), and regressor orthogonalization with respect to the stimulus protocol to separate systematic differences from independent fluctuations (Feige et al., 2005; Mulert et al., 2010).

Finally, apart from rhythmic fluctuations and ERPs, other more context-specific EEG features have also been explored, such as brief sleep phenomena captured during non-rapid eye movement stages (Laufs et al., 2007). Epilepsy studies, where concurrent EEG–fMRI has its roots, have strongly benefitted from EEG-based prediction approaches, and a substantial amount of work has been dedicated to this application. The temporal dynamics of epileptic activity can be captured with EEG and converted into meaningful BOLD predictors, allowing for a more precise spatial localization of neuronal generators and propagation networks (Gotman and Pittau, 2011). Typically, interictal spikes and ictal events are described by boxcar functions, eventually split into different classes or phases, and convolved with an appropriate HRF (Murta et al., 2012; Thornton et al., 2010; Tyvaert et al., 2008). As an example, Tyvaert et al. (2008) investigated the brain regions involved in ictal and interictal activity in patients with different types of cortical malformations. First, ictal and interictal events were identified through visual inspection by the neurophysiologist, selectively grouped, and used to design boxcar timecourses. In order to account for different response latencies, each timecourse was then convolved with several

HRFs of varying peak lags, originating a set of multi-lagged regressors to include in a global GLM. Other approaches have also been proposed for the extraction of EEG timecourses representative of the epileptic activity of interest, based on ICA decomposition (Formaggio et al., 2011; Marques et al., 2009) or continuous electrical source imaging (Vulliemoz et al., 2010). Grouiller et al. (2011) proposed to build "epilepsy-specific maps" based on the EEG field power topographies generated during interictal activity, as measured in off-scanner recordings. These were then correlated with field topographies from simultaneous EEG–fMRI data, and the timecourse of the resulting correlation coefficient was used as a GLM regressor. Analogous approaches were proposed by Britz et al. (2010) and Yuan et al. (2012) to study the BOLD correlates of EEG microstates.

Data integration: symmetrical approaches

In contrast with asymmetrical approaches, which tend to rely on the assumption that the two modalities probe coincident neuronal substrates, symmetrical approaches explicitly recognize EEG and fMRI signals as measures of distinct, only partially overlapping substrates of neuronal activity. These approaches establish a bilateral dependence between EEG and fMRI (Rosa et al., 2010a), and can be grouped into two main categories: data-driven and model-based (Fig. 2).

Data-driven methods

Data-driven symmetrical integration techniques avoid the need to model the complex neuronal population and neurovascular coupling dynamics. In an early work centered on EEG rhythms, Martinez-Montes et al. (2004) modeled fMRI and EEG signals as multidimensional patterns composed of "atoms", with specific signatures in space, time, and (for EEG) frequency. Space and frequency signatures were estimated by multiway partial least-squares regression, which imposed maximal covariance between the time signatures of the two modalities. This yielded EEG spectral and spatial signatures with time-varying envelopes that covaried maximally with the fluctuations of BOLD topographies.

Others have opted for Bayesian formulations for the problem of estimating common and modality-specific substrates, reflecting instances of EEG–fMRI coupling and uncoupling. Daunizeau et al. (2007) considered a finite parceling of the cortical surface into a set of functionally homogeneous clusters, and modeled EEG and BOLD signals as linear systems with respect to the distributed cortical dipoles and HRF. Spatial and temporal smoothness priors were specified for this multimodal hierarchical model, and a variational learning scheme was applied to iteratively estimate its posterior probability density function. In a latter study, Luessi et al. (2011) extended this method with more flexible smoothness assumptions, allowing for sharper activation boundaries and spatially adaptive temporal constraints. In a different approach, Lei et al. (2011) used Bayesian-formulated criteria to match functional networks obtained separately for each modality by spatial ICA, whereby fMRI networks were introduced as covariance priors to reconstruct the sources of EEG networks. Functional connectivity between common, EEG-specific and fMRI-specific sources was then analyzed with graph theory and Granger causality methods.

Another integration approach of growing interest is that of joint ICA, initially proposed by Calhoun et al. (2006) to merge individual fMRI and ERP data on a multi-subject scale. It was assumed that EEG independent temporal components and fMRI independent spatial components were linearly combined across subjects by the same mixing matrix, allowing trial-averaged ERP timecourses and BOLD activation maps to be concatenated in a single data vector per subject. ICA was then applied to the resulting global observation matrix, to determine the underlying BOLD-ERP components that were combined to form individual subject responses. Subsequent studies centered on this approach addressed the assumption that the independent sources from both modalities undergo the same linear covariation across subjects (Calhoun et al., 2009), proposed additional steps for data normalization and reduction (Moosmann et al., 2008), and assessed the robustness of the method (Mijovic et al., 2012).

In recent years, various other heuristic methods have been proposed. Ostwald et al. (2010) analyzed diverse features of EEG and fMRI responses in an information theoretic framework. Under visual stimulation, bimodal stimulus–response probability distributions were estimated for the features of interest, and measures such as mutual information and synergy were applied to assess the amount of information shared by the two modalities with the stimuli and between each other. This framework, later improved with more powerful data selection and statistical evaluation steps (Ostwald et al., 2011), avoided the stronger assumptions inherent to linear regression and a priori HRF modeling. A similar approach was later applied to epilepsy patients, where interictal epileptic activity was included as a relevant EEG feature (Caballero-Gaudes et al., 2013). Yang et al. (2010) presented a reciprocal approach combining EEG-based fMRI prediction with fMRI-driven EEG estimation. EEG data were initially decomposed with ICA, and the timecourses of the independent components were used for fMRI GLM analysis. Each of the resulting statistical maps was then used as a prior to reconstruct the EEG sources originating the corresponding independent component, yielding a final source distribution with improved spatiotemporal resolution. Correa et al. (2010) used multi-set canonical correlation analysis to evaluate multi-subject trial-by-trial covariations between fMRI maps and ERPs. This yielded a data decomposition where the cross-modality correlation in trial-by-trial variations was maximized, along with the correlations within and between modalities across subjects. As another example, De Martino et al. (2011) used multivariate relevance vector machine regression to learn the trial-by-trial coupling between single-trial EEG timecourses and the corresponding BOLD volumes.

Model-based integration

Model-based symmetrical approaches have addressed the integration problem through the development of increasingly more realistic biophysical models describing the neuronal, metabolic, and hemodynamic processes underlying EEG and BOLD signals, continuously improved with information from brain architecture and function at diverse spatial scales (Rosa et al., 2010a). The full modeling challenge can be decomposed into several interacting parts, including: 1) the neuronal response to external stimulation, neuronal population dynamics and interactions; 2) the propagation of electromagnetic fluctuations to the scalp; and 3) the coupling between neuronal activity, $CMRO_2$ and CBF, the vascular mechanisms relating dHb concentration, CBF and CBV, and the BOLD signal dependence thereon (Buxton et al., 2004; Deneux and Faugeras, 2010; Riera et al., 2006).

Neuronal population responses and interactions pose a remarkable modeling challenge. While single-neuron responses can be satisfactorily described by fairly simple models, neuronal populations can express complex, rhythmic and transient patterns of excitatory and inhibitory interactions (Lauritzen and Gold, 2003; Logothetis, 2008). In an early work modeling both the neuronal and hemodynamic responses to stimulation, Buxton et al. (2004) proposed a simple inhibitory feedback system to describe the local neuronal response as a balance between excitatory and inhibitory inputs. This model could reproduce neuronal adaptation, post-stimulus undershooting and "refractory" effects, and could be applied to either synaptic or spiking activity, depending on which was considered the primary driver of local changes (Rosa et al., 2011). In parallel, more biophysically-inspired approaches were continuously developed. Jansen and Rit (1995) proposed a model for a single cortical column comprising a population of excitatory pyramidal cells, receiving inhibitory feedback from local interneurons and excitatory input from stellate cells. Babajani and Soltanian-Zadeh (2006) extended this model by joining multiple cortical columns to form a cortical area, introducing anatomically-plausible interactions between pyramidal cell groups and neighboring column cells. More recently, the model was further extended to describe multiple cortical areas, interacting

through long-range connections based on pyramidal cell output (Babajani-Feremi and Soltanian-Zadeh, 2010).

Following neuronal responses, the link to measurable scalp EEG fluctuations can be established through a forward model of head volume conduction (Hamalainen and Sarvas, 1989), which can be treated as a linear system (Dale and Sereno, 1993; Lenz et al., 2011). For BOLD signals, however, the link to neuronal activity is mediated by a complex cascade of metabolic and hemodynamic processes governing $CMRO_2$, CBF and CBV changes (Buxton et al., 1998; Davis et al., 1998), of which many aspects remain unclear (Riera and Sumiyoshi, 2010).

In an early work, Friston et al. (2000) proposed a linear relationship between CBF and synaptic activity, described by a set of differential equations that included coupling efficacy and signal decay effects, and auto-regulatory feedback from blood flow itself. Riera et al. (2006) modeled the arterial input from neurons as a lowpass-filtered version of the local concentration of nitric oxide (NO), a major regulatory intermediate for vascular control. Sotero and Trujillo-Barreto (2007) built a model linking neuronal activity to CBF and $CMRO_2$ which differentiated the effect of excitatory and inhibitory synaptic activity on the metabolic paths of neurotransmitter cycling, leading to differences in O_2 consumption. Additionally, only excitatory activity exerted a direct influence on CBF. This model was later extended to multiple cortical areas by introducing short- and long-range interactions between populations (Sotero and Trujillo-Barreto, 2008).

For a complete description of BOLD dynamics, CBV changes in response to CBF and $CMRO_2$ fluctuations must also be considered. In the so-called balloon model, Buxton et al. (1998) assumed that CBV changes occur primarily in the venous compartment, modeled as a balloon fed by the capillary bed output. Inward flow increases would raise the pressure inside the compartment, driving increases in outward flow. This was stated as an equation relating inward and outward blood flow with blood volume, and the local dHb concentration was added as a function of CBV, inward and outward flows, and $CMRO_2$. Mandeville et al. (1999) applied windkessel theory to extend the balloon model with a resistive description of brain vasculature, to model capillary and venous compliance. This extended model has been integrated in the vast majority of subsequent studies, often with additional modifications (Boas et al., 2008; Zheng et al., 2002).

A final note is dedicated to the problem of model inversion. Adding to the ill-posed nature of neuronal source reconstruction, the biophysical models discussed involve complex cascades of dynamic systems, usually formulated as differential equation sets with large numbers of free parameters (Deneux and Faugeras, 2010; Friston et al., 2000). As models become increasingly more detailed, and grow from single mini-columns to multiple cortical areas, inversion algorithms suffer inevitable increases in numerical complexity and computational burden (Rosa et al., 2010a). Indeed, the problem of biophysical model inversion has become a field of research of its own (Friston et al., 2008; Lenz et al., 2011; Moran et al., 2007; Riera et al., 2007; Valdes-Sosa et al., 2009).

Conclusions

In this review, we have covered some of the major contributions to the integrated analysis of EEG and fMRI data for the study of human brain function. The advantages and pitfalls of different approaches were treated in the light of the strengths and limitations of the two modalities themselves, and some of the most important ideas proposed in the literature were described.

As has been seen, EEG–fMRI integration poses remarkable methodological and conceptual challenges which have been the object of intense research over the last two decades, spanning a wide variety of approaches in both the acquisition and analysis domains. Depending on the scientific question at hand, one should choose the most suitable approach according to the expected spatiotemporal patterns and possible confounds. Conversely, a poor knowledge of the strengths and limitations of each approach, as well as the intrinsic properties of EEG and fMRI signals themselves, may lead to erroneous interpretations of the data. A solid background of both individual modalities and integration approaches is essential for choosing the best experimental and analysis strategy, and extracting reliable conclusions.

Unsurprisingly, the development of EEG–fMRI integration methodologies has evolved hand-in-hand with the discovery of increasingly finer functional features. EEG-driven fMRI approaches have shown meaningful relationships between fluctuations in EEG power, frequency or phase and local BOLD changes, while fMRI-driven EEG approaches have achieved enhanced neuronal source reconstructions. As both separate and joint technical capabilities of the two modalities continue to improve, new features will undoubtedly be encountered, providing fresh insights and new questions. Concurrently, improved computational methods and novel results from parallel neurophysiology studies will provide richer measurements and more accurate biophysical constraints to guide neurovascular model design, leading to larger-scale, more detailed and more accurate descriptions of the brain. Indeed, integrated EEG–fMRI is likely to remain one of the most powerful tools available for the non-invasive study of human brain function, with new scientific landmarks yet to be achieved.

Acknowledgments

This work was supported by Centre d'Imagerie BioMédicale (CIBM) of the UNIL, UNIGE, HUG, CHUV, EPFL and the Leenaards and Jeantet Foundations, and by the Portuguese Science Foundation (FCT) through grants SFRH/BD/51449/2011, PTDC/SAU-ENB/112294/2009 and PEst-OE/EEI/LA0009/2011.

Conflict of interest

The authors have no conflicts of interest regarding this paper.

References

Ahlfors, S.P., Simpson, G.V., 2004. Geometrical interpretation of fMRI-guided MEG/EEG inverse estimates. NeuroImage 22, 323–332.
Allen, P.J., Polizzi, G., Krakow, K., Fish, D.R., Lemieux, L., 1998. Identification of EEG events in the MR scanner: the problem of pulse artifact and a method for its subtraction. NeuroImage 8, 229–239.
Allen, P.J., Josephs, O., Turner, R., 2000. A method for removing imaging artifact from continuous EEG recorded during functional MRI. NeuroImage 12, 230–239.
Arthurs, O.J., Donovan, T., Spiegelhalter, D.J., Pickard, J.D., Boniface, S.J., 2007. Intracortically distributed neurovascular coupling relationships within and between human somatosensory cortices. Cereb. Cortex 17, 661–668.
Attwell, D., Buchan, A.M., Charpak, S., Lauritzen, M., Macvicar, B.A., Newman, E.A., 2010. Glial and neuronal control of brain blood flow. Nature 468, 232–243.
Babajani, A., Soltanian-Zadeh, H., 2006. Integrated MEG/EEG and fMRI model based on neural masses. IEEE Trans. Biomed. Eng. 53, 1794–1801.
Babajani-Feremi, A., Soltanian-Zadeh, H., 2010. Multi-area neural mass modeling of EEG and MEG signals. NeuroImage 52, 793–811.
Babiloni, F., Mattia, D., Babiloni, C., Astolfi, L., Salinari, S., Basilisco, A., Rossini, P.M., Marciani, M.G., Cincotti, F., 2004. Multimodal integration of EEG, MEG and fMRI data for the solution of the neuroimage puzzle. Magn. Reson. Imaging 22, 1471–1476.
Babiloni, F., Cincotti, F., Babiloni, C., Carducci, F., Mattia, D., Astolfi, L., Basilisco, A., Rossini, P.M., Ding, L., Ni, Y., Cheng, J., Christine, K., Sweeney, J., He, B., 2005. Estimation of the cortical functional connectivity with the multimodal integration of high-resolution EEG and fMRI data by directed transfer function. NeuroImage 24, 118–131.
Becker, R., Reinacher, M., Freyer, F., Villringer, A., Ritter, P., 2011. How ongoing neuronal oscillations account for evoked fMRI variability. J. Neurosci. 31, 11016–11027.
Benar, C.G., Schon, D., Grimault, S., Nazarian, B., Burle, B., Roth, M., Badier, J.M., Marquis, P., Liegeois-Chauvel, C., Anton, J.L., 2007. Single-trial analysis of oddball event-related potentials in simultaneous EEG–fMRI. Hum. Brain Mapp. 28, 602–613.
Biswal, B., Yetkin, F.Z., Haughton, V.M., Hyde, J.S., 1995. Functional connectivity in the motor cortex of resting human brain using echo-planar MRI. Magn. Reson. Med. 34, 537–541.
Bledowski, C., Prvulovic, D., Hoechstetter, K., Scherg, M., Wibral, M., Goebel, R., Linden, D.E., 2004. Localizing P300 generators in visual target and distractor processing: a combined event-related potential and functional magnetic resonance imaging study. J. Neurosci. 24, 9353–9360.
Boas, D.A., Jones, S.R., Devor, A., Huppert, T.J., Dale, A.M., 2008. A vascular anatomical network model of the spatio-temporal response to brain activation. NeuroImage 40, 1116–1129.

Boly, M., Balteau, E., Schnakers, C., Degueldre, C., Moonen, G., Luxen, A., Phillips, C., Peigneux, P., Maquet, P., Laureys, S., 2007. Baseline brain activity fluctuations predict somatosensory perception in humans. Proc. Natl. Acad. Sci. U. S. A. 104, 12187–12192.
Bonmassar, G., Anami, K., Ives, J., Belliveau, J.W., 1999. Visual evoked potential (VEP) measured by simultaneous 64-channel EEG and 3 T fMRI. Neuroreport 10, 1893–1897.
Bonmassar, G., Purdon, P.L., Jaaskelainen, I.P., Chiappa, K., Solo, V., Brown, E.N., Belliveau, J.W., 2002. Motion and ballistocardiogram artifact removal for interleaved recording of EEG and EPs during MRI. NeuroImage 16, 1127–1141.
Brass, M., Ullsperger, M., Knoesche, T.R., von Cramon, D.Y., Phillips, N.A., 2005. Who comes first? The role of the prefrontal and parietal cortex in cognitive control. J. Cogn. Neurosci. 17, 1367–1375.
Bridwell, D.A., Wu, L., Eichele, T., Calhoun, V.D., 2012. The spatiospectral characterization of brain networks: fusing concurrent EEG spectra and fMRI maps. NeuroImage 69C, 101–111.
Britz, J., Van De Ville, D., Michel, C.M., 2010. BOLD correlates of EEG topography reveal rapid resting-state network dynamics. NeuroImage 52, 1162–1170.
Brown, G.D., Yamada, S., Sejnowski, T.J., 2001. Independent component analysis at the neural cocktail party. Trends Neurosci. 24, 54–63.
Busch, N.A., Dubois, J., VanRullen, R., 2009. The phase of ongoing EEG oscillations predicts visual perception. J. Neurosci. 29, 7869–7876.
Buxton, R.B., Wong, E.C., Frank, L.R., 1998. Dynamics of blood flow and oxygenation changes during brain activation: the balloon model. Magn. Reson. Med. 39, 855–864.
Buxton, R.B., Uludag, K., Dubowitz, D.J., Liu, T.T., 2004. Modeling the hemodynamic response to brain activation. NeuroImage 23 (Suppl. 1), S220–S233.
Caballero-Gaudes, C., Van de Ville, D., Grouiller, F., Thornton, R., Lemieux, L., Seeck, M., Lazeyras, F., Vulliemoz, S., 2013. Mapping interictal epileptic discharges using mutual information between concurrent EEG and fMRI. NeuroImage 68, 248–262.
Calhoun, V.D., Adali, T., Pearlson, G.D., Kiehl, K.A., 2006. Neuronal chronometry of target detection: fusion of hemodynamic and event-related potential data. NeuroImage 30, 544–553.
Calhoun, V.D., Liu, J., Adali, T., 2009. A review of group ICA for fMRI data and ICA for joint inference of imaging, genetic, and ERP data. NeuroImage 45, S163–S172.
Carmichael, D.W., Vulliemoz, S., Rodionov, R., Walker, M., Rosenkranz, K., McEvoy, A., Lemieux, L., 2011. Simultaneous intracranial EEG–fMRI in humans suggests that high gamma frequencies are the closest neurophysiological correlate of BOLD fMRI. 19th Annual Meeting of the International Society for Magnetic Resonance in Medicine, Montréal, Canada.
Correa, N.M., Eichele, T., Adali, T., Li, Y.O., Calhoun, V.D., 2010. Multi-set canonical correlation analysis for the fusion of concurrent single trial ERP and functional MRI. NeuroImage 50, 1438–1445.
Cunningham, C.B., Goodyear, B.G., Badawy, R., Zaamout, F., Pittman, D.J., Beers, C.A., Federico, P., 2012. Intracranial EEG–fMRI analysis of focal epileptiform discharges in humans. Epilepsia 53, 1636–1648.
Dale, A.M., Halgren, E., 2001. Spatiotemporal mapping of brain activity by integration of multiple imaging modalities. Curr. Opin. Neurobiol. 11, 202–208.
Dale, A.M., Sereno, M.I., 1993. Improved localization of cortical activity by combining EEG and MEG with MRI cortical surface reconstruction: a linear approach. J. Cogn. Neurosci. 5, 162–176.
Dale, A.M., Liu, A.K., Fischl, B.R., Buckner, R.L., Belliveau, J.W., Lewine, J.D., Halgren, E., 2000. Dynamic statistical parametric mapping: combining fMRI and MEG for high-resolution imaging of cortical activity. Neuron 26, 55–67.
Daunizeau, J., Grova, C., Mattout, J., Marrelec, G., Clonda, D., Goulard, B., Pelegrini-Issac, M., Lina, J.M., Benali, H., 2005. Assessing the relevance of fMRI-based prior in the EEG inverse problem: a Bayesian model comparison approach. IEEE Trans. Signal Process. 53, 3461–3472.
Daunizeau, J., Grova, C., Marrelec, G., Mattout, J., Jbabdi, S., Pelegrini-Issac, M., Lina, J.M., Benali, H., 2007. Symmetrical event-related EEG/fMRI information fusion in a variational Bayesian framework. NeuroImage 36, 69–87.
Davis, T.L., Kwong, K.K., Weisskoff, R.M., Rosen, B.R., 1998. Calibrated functional MRI: mapping the dynamics of oxidative metabolism. Proc. Natl. Acad. Sci. U. S. A. 95, 1834–1839.
De Martino, F., de Borst, A.W., Valente, G., Goebel, R., Formisano, E., 2011. Predicting EEG single trial responses with simultaneous fMRI and relevance vector machine regression. NeuroImage 56, 826–836.
de Munck, J.C., Goncalves, S.I., Huijboom, L., Kuijer, J.P., Pouwels, P.J., Heethaar, R.M., Lopes da Silva, F.H., 2007. The hemodynamic response of the alpha rhythm: an EEG/fMRI study. NeuroImage 35, 1142–1151.
de Munck, J.C., Goncalves, S.I., Faes, T.J., Kuijer, J.P., Pouwels, P.J., Heethaar, R.M., Lopes da Silva, F.H., 2008. A study of the brain's resting state based on alpha band power, heart rate and fMRI. NeuroImage 42, 112–121.
de Munck, J.C., Goncalves, S.I., Mammoliti, R., Heethaar, R.M., Lopes da Silva, F.H., 2009. Interactions between different EEG frequency bands and their effect on alpha-fMRI correlations. NeuroImage 47, 69–76.
Debener, S., Kranczioch, C., Herrmann, C.S., Engel, A.K., 2002. Auditory novelty oddball allows reliable distinction of top–down and bottom–up processes of attention. Int. J. Psychophysiol. 46, 77–84.
Debener, S., Ullsperger, M., Siegel, M., Fiehler, K., von Cramon, D.Y., Engel, A.K., 2005. Trial-by-trial coupling of concurrent electroencephalogram and functional magnetic resonance imaging identifies the dynamics of performance monitoring. J. Neurosci. 25, 11730–11737.
Debener, S., Ullsperger, M., Siegel, M., Engel, A.K., 2006. Single-trial EEG–fMRI reveals the dynamics of cognitive function. Trends Cogn. Sci. 10, 558–563.
Debener, S., Mullinger, K.J., Niazy, R.K., Bowtell, R.W., 2008. Properties of the ballistocardiogram artefact as revealed by EEG recordings at 1.5, 3 and 7 T static magnetic field strength. Int. J. Psychophysiol. 67, 189–199.
Delorme, A., Makeig, S., 2004. EEGLAB: an open source toolbox for analysis of single-trial EEG dynamics including independent component analysis. J. Neurosci. Methods 134, 9–21.
Deneux, T., Faugeras, O., 2010. EEG–fMRI fusion of paradigm-free activity using Kalman filtering. Neural Comput. 22, 906–948.
Eichele, T., Specht, K., Moosmann, M., Jongsma, M.L., Quiroga, R.Q., Nordby, H., Hugdahl, K., 2005. Assessing the spatiotemporal evolution of neuronal activation with single-trial event-related potentials and functional MRI. Proc. Natl. Acad. Sci. U. S. A. 102, 17798–17803.
Eichele, T., Calhoun, V.D., Moosmann, M., Specht, K., Jongsma, M.L., Quiroga, R.Q., Nordby, H., Hugdahl, K., 2008. Unmixing concurrent EEG–fMRI with parallel independent component analysis. Int. J. Psychophysiol. 67, 222–234.
Feige, B., Scheffler, K., Esposito, F., Di Salle, F., Hennig, J., Seifritz, E., 2005. Cortical and subcortical correlates of electroencephalographic alpha rhythm modulation. J. Neurophysiol. 93, 2864–2872.
Formaggio, E., Storti, S.F., Bertoldo, A., Manganotti, P., Fiaschi, A., Toffolo, G.M., 2011. Integrating EEG and fMRI in epilepsy. NeuroImage 54, 2719–2731.
Fox, M.D., Raichle, M.E., 2007. Spontaneous fluctuations in brain activity observed with functional magnetic resonance imaging. Nat. Rev. Neurosci. 8, 700–711.
Freyer, F., Becker, R., Anami, K., Curio, G., Villringer, A., Ritter, P., 2009. Ultrahigh-frequency EEG during fMRI: pushing the limits of imaging-artifact correction. NeuroImage 48, 94–108.
Friston, K.J., Fletcher, P., Josephs, O., Holmes, A., Rugg, M.D., Turner, R., 1998. Event-related fMRI: characterizing differential responses. NeuroImage 7, 30–40.
Friston, K.J., Mechelli, A., Turner, R., Price, C.J., 2000. Nonlinear responses in fMRI: the Balloon model, Volterra kernels, and other hemodynamics. NeuroImage 12, 466–477.
Friston, K.J., Trujillo-Barreto, N., Daunizeau, J., 2008. DEM: a variational treatment of dynamic systems. NeuroImage 41, 849–885.
Garreffa, G., Bianciardi, M., Hagberg, G.E., Macaluso, E., Marciani, M.G., Maraviglia, B., Abbafati, M., Carni, M., Bruni, I., Bianchi, L., 2004. Simultaneous EEG–fMRI acquisition: how far is it from being a standardized technique? Magn. Reson. Imaging 22, 1445–1455.
Giraud, A.L., Kleinschmidt, A., Poeppel, D., Lund, T.E., Frackowiak, R.S., Laufs, H., 2007. Endogenous cortical rhythms determine cerebral specialization for speech perception and production. Neuron 56, 1127–1134.
Goense, J., Merkle, H., Logothetis, N.K., 2012. High-resolution fMRI reveals laminar differences in neurovascular coupling between positive and negative BOLD responses. Neuron 76, 629–639.
Goldman, R.I., Stern, J.M., Engel Jr., J., Cohen, M.S., 2000. Acquiring simultaneous EEG and functional MRI. Clin. Neurophysiol. 111, 1974–1980.
Goldman, R.I., Stern, J.M., Engel Jr., J., Cohen, M.S., 2002. Simultaneous EEG and fMRI of the alpha rhythm. Neuroreport 13, 2487–2492.
Goncalves, S.I., de Munck, J.C., Pouwels, P.J., Schoonhoven, R., Kuijer, J.P., Maurits, N.M., Hoogduin, J.M., Van Someren, E.J., Heethaar, R.M., Lopes da Silva, F.H., 2006. Correlating the alpha rhythm to BOLD using simultaneous EEG/fMRI: inter-subject variability. NeuroImage 30, 203–213.
Gotman, J., Pittau, F., 2011. Combining EEG and fMRI in the study of epileptic discharges. Epilepsia 52 (Suppl. 4), 38–42.
Grouiller, F., Vercueil, L., Krainik, A., Segebarth, C., Kahane, P., David, O., 2007. A comparative study of different artefact removal algorithms for EEG signals acquired during functional MRI. NeuroImage 38, 124–137.
Grouiller, F., Vercueil, L., Krainik, A., Segebarth, C., Kahane, P., David, O., 2010. Characterization of the hemodynamic modes associated with interictal epileptic activity using a deformable model-based analysis of combined EEG and functional MRI recordings. Hum. Brain Mapp. 31, 1157–1173.
Grouiller, F., Thornton, R.C., Groening, K., Spinelli, L., Duncan, J.S., Schaller, K., Siniatchkin, M., Lemieux, L., Seeck, M., Michel, C.M., Vulliemoz, S., 2011. With or without spikes: localization of focal epileptic activity by simultaneous electroencephalography and functional magnetic resonance imaging. Brain 134, 2867–2886.
Hamalainen, M.S., Sarvas, J., 1989. Realistic conductivity geometry model of the human head for interpretation of neuromagnetic data. IEEE Trans. Biomed. Eng. 36, 165–171.
Harvey, B.M., Vansteensel, M.J., Ferrier, C.H., Petridou, N., Zuiderbaan, W., Aarnoutse, E.J., Bleichner, M.G., Dijkerman, H.C., van Zandvoort, M.J., Leijten, F.S., Ramsey, N.F., Dumoulin, S.O., 2013. Frequency specific spatial interactions in human electrocorticography: V1 alpha oscillations reflect surround suppression. NeuroImage 65, 424–432.
Heinze, H.J., Mangun, G.R., Burchert, W., Hinrichs, H., Scholz, M., Munte, T.F., Gos, A., Scherg, M., Johannes, S., Hundeshagen, H., et al., 1994. Combined spatial and temporal imaging of brain activity during visual selective attention in humans. Nature 372, 543–546.
Hermes, D., Miller, K.J., Vansteensel, M.J., Aarnoutse, E.J., Leijten, F.S., Ramsey, N.F., 2012. Neurophysiologic correlates of fMRI in human motor cortex. Hum. Brain Mapp. 33, 1689–1699.
Herrmann, C.S., Debener, S., 2008. Simultaneous recording of EEG and BOLD responses: a historical perspective. Int. J. Psychophysiol. 67, 161–168.
Hinterberger, T., Veit, R., Wilhelm, B., Weiskopf, N., Vatine, J.J., Birbaumer, N., 2005. Neuronal mechanisms underlying control of a brain–computer interface. Eur. J. Neurosci. 21, 3169–3181.
Horovitz, S.G., Rossion, B., Skudlarski, P., Gore, J.C., 2004. Parametric design and correlational analyses help integrating fMRI and electrophysiological data during face processing. NeuroImage 22, 1587–1595.
HuangHellinger, F.R., Breiter, H.C., McCormack, G., Cohen, M.S., Kwong, K.K., Sutton, J.P., Savoy, R.L., Weisskoff, R.M., Davis, T.L., Baker, J.R., Belliveau, J.W., Rosen, B.R., 1995. Simultaneous functional magnetic resonance imaging and electrophysiological recording. Hum. Brain Mapp. 3, 13–23.

Im, C.H., Jung, H.K., Fujimaki, N., 2005. fMRI-constrained MEG source imaging and consideration of fMRI invisible sources. Hum. Brain Mapp. 26, 110–118.
Ives, J.R., Warach, S., Schmitt, F., Edelman, R.R., Schomer, D.L., 1993. Monitoring the patient's EEG during echo planar MRI. Electroencephalogr. Clin. Neurophysiol. 87, 417–420.
Jann, K., Dierks, T., Boesch, C., Kottlow, M., Strik, W., Koenig, T., 2009. BOLD correlates of EEG alpha phase-locking and the fMRI default mode network. NeuroImage 45, 903–916.
Jansen, B.H., Rit, V.G., 1995. Electroencephalogram and visual evoked potential generation in a mathematical model of coupled cortical columns. Biol. Cybern. 73, 357–366.
Jaspers-Fayer, F., Ertl, M., Leicht, G., Leupelt, A., Mulert, C., 2012. Single-trial EEG–fMRI coupling of the emotional auditory early posterior negativity. NeuroImage 62, 1807–1814.
Jefferys, J.G., Menendez de la Prida, L., Wendling, F., Bragin, A., Avoli, M., Timofeev, I., Lopes da Silva, F.H., 2012. Mechanisms of physiological and epileptic HFO generation. Prog. Neurobiol. 98, 250–264.
Jezzard, P., Matthews, P.M., Smith, S.M., NetLibrary, I., 2001. Functional MRI: An Introduction to Methods. Oxford University Press, Oxford, New York.
Jorge, J., Figueiredo, P., van der Zwaag, W., Marques, J.P., 2013. Signal fluctuations in fMRI data acquired with 2D-EPI and 3D-EPI at 7 Tesla. Magn. Reson. Imaging 31, 212–220.
Katscher, U., Voigt, T., Findeklee, C., Vernickel, P., Nehrke, K., Dossel, O., 2009. Determination of electric conductivity and local SAR via B1 mapping. IEEE Trans. Med. Imaging 28, 1365–1374.
Khader, P., Schicke, T., Roder, B., Rosler, F., 2008. On the relationship between slow cortical potentials and BOLD signal changes in humans. Int. J. Psychophysiol. 67, 252–261.
Kilner, J.M., Mattout, J., Henson, R., Friston, K.J., 2005. Hemodynamic correlates of EEG: a heuristic. NeuroImage 28, 280–286.
Kottlow, M., Jann, K., Dierks, T., Koenig, T., 2012. Increased phase synchronization during continuous face integration measured simultaneously with EEG and fMRI. Clin. Neurophysiol. 123, 1536–1548.
Krakow, K., Woermann, F.G., Symms, M.R., Allen, P.J., Lemieux, L., Barker, G.J., Duncan, J.S., Fish, D.R., 1999. EEG-triggered functional MRI of interictal epileptiform activity in patients with partial seizures. Brain 122 (Pt 9), 1679–1688.
Kruger, G., Kastrup, A., Glover, G.H., 2001. Neuroimaging at 1.5 T and 3.0 T: comparison of oxygenation-sensitive magnetic resonance imaging. Magn. Reson. Med. 45, 595–604.
Kruggel, F., Wiggins, C.J., Herrmann, C.S., von Cramon, D.Y., 2000. Recording of the event-related potentials during functional MRI at 3.0 Tesla field strength. Magn. Reson. Med. 44, 277–282.
Lachaux, J.P., Fonlupt, P., Kahane, P., Minotti, L., Hoffmann, D., Bertrand, O., Baciu, M., 2007. Relationship between task-related gamma oscillations and BOLD signal: new insights from combined fMRI and intracranial EEG. Hum. Brain Mapp. 28, 1368–1375.
Laufs, H., 2012. A personalized history of EEG–fMRI integration. NeuroImage 62, 1056–1067.
Laufs, H., Kleinschmidt, A., Beyerle, A., Eger, E., Salek-Haddadi, A., Preibisch, C., Krakow, K., 2003. EEG-correlated fMRI of human alpha activity. NeuroImage 19, 1463–1476.
Laufs, H., Holt, J.L., Elfont, R., Krams, M., Paul, J.S., Krakow, K., Kleinschmidt, A., 2006. Where the BOLD signal goes when alpha EEG leaves. NeuroImage 31, 1408–1418.
Laufs, H., Walker, M.C., Lund, T.E., 2007. Brain activation and hypothalamic functional connectivity during human non-rapid eye movement sleep: an EEG/fMRI study—its limitations and an alternative approach. Brain 130, e75 (author reply e76).
Lauritzen, M., Gold, L., 2003. Brain function and neurophysiological correlates of signals used in functional neuroimaging. J. Neurosci. 23, 3972–3980.
Lei, X., Ostwald, D., Hu, J., Qiu, C., Porcaro, C., Bagshaw, A.P., Yao, D., 2011. Multimodal functional network connectivity: an EEG–fMRI fusion in network space. PLoS One 6, e24642.
Leite, M., Leal, A., Figueiredo, P., 2013. Transfer function between EEG and BOLD signals of epileptic activity. Front. Neurol. 4.
Lemieux, L., McBride, A., Hand, J.W., 1996. Calculation of electrical potentials on the surface of a realistic head model by finite differences. Phys. Med. Biol. 41, 1079–1091.
Lemieux, L., Allen, P.J., Franconi, F., Symms, M.R., Fish, D.R., 1997. Recording of EEG during fMRI experiments: patient safety. Magn. Reson. Med. 38, 943–952.
Lemieux, L., Salek-Haddadi, A., Josephs, O., Allen, P., Toms, N., Scott, C., Krakow, K., Turner, R., Fish, D.R., 2001. Event-related fMRI with simultaneous and continuous EEG: description of the method and initial case report. NeuroImage 14, 780–787.
Lenz, M., Musso, M., Linke, Y., Tuscher, O., Timmer, J., Weiller, C., Schelter, B., 2011. Joint EEG/fMRI state space model for the detection of directed interactions in human brains—a simulation study. Physiol. Meas. 32, 1725–1736.
Liu, Z., He, B., 2008. fMRI–EEG integrated cortical source imaging by use of time-variant spatial constraints. NeuroImage 39, 1198–1214.
Liu, T.T., Frank, L.R., Wong, E.C., Buxton, R.B., 2001. Detection power, estimation efficiency, and predictability in event-related fMRI. NeuroImage 13, 759–773.
Liu, Z., Zhang, N., Chen, W., He, B., 2009. Mapping the bilateral visual integration by EEG and fMRI. NeuroImage 46, 989–997.
Liu, Z., Rios, C., Zhang, N., Yang, L., Chen, W., He, B., 2010. Linear and nonlinear relationships between visual stimuli, EEG and BOLD fMRI signals. NeuroImage 50, 1054–1066.
Logothetis, N.K., 2002. The neural basis of the blood-oxygen-level-dependent functional magnetic resonance imaging signal. Philos. Trans. R. Soc. Lond. B Biol. Sci. 357, 1003–1037.
Logothetis, N.K., 2008. What we can do and what we cannot do with fMRI. Nature 453, 869–878.
Logothetis, N.K., Pauls, J., Augath, M., Trinath, T., Oeltermann, A., 2001. Neurophysiological investigation of the basis of the fMRI signal. Nature 412, 150–157.
Luessi, M., Babacan, S.D., Molina, R., Booth, J.R., Katsaggelos, A.K., 2011. Bayesian symmetrical EEG/fMRI fusion with spatially adaptive priors. NeuroImage 55, 113–132.
Mandelkow, H., Halder, P., Boesiger, P., Brandeis, D., 2006. Synchronization facilitates removal of MRI artefacts from concurrent EEG recordings and increases usable bandwidth. NeuroImage 32, 1120–1126.
Mandeville, J.B., Marota, J.J., Ayata, C., Zaharchuk, G., Moskowitz, M.A., Rosen, B.R., Weisskoff, R.M., 1999. Evidence of a cerebrovascular postarteriole windkessel with delayed compliance. J. Cereb. Blood Flow Metab. 19, 679–689.
Mantini, D., Perrucci, M.G., Del Gratta, C., Romani, G.L., Corbetta, M., 2007. Electrophysiological signatures of resting state networks in the human brain. Proc. Natl. Acad. Sci. U. S. A. 104, 13170–13175.
Marques, J.P., Rebola, J., Figueiredo, P., Pinto, A., Sales, F., Castelo-Branco, M., 2009. ICA decomposition of EEG signal for fMRI processing in epilepsy. Hum. Brain Mapp. 30, 2986–2996.
Martinez, A., Anllo-Vento, L., Sereno, M.I., Frank, L.R., Buxton, R.B., Dubowitz, D.J., Wong, E.C., Hinrichs, H., Heinze, H.J., Hillyard, S.A., 1999. Involvement of striate and extrastriate visual cortical areas in spatial attention. Nat. Neurosci. 2, 364–369.
Martinez-Montes, E., Valdes-Sosa, P.A., Miwakeichi, F., Goldman, R.I., Cohen, M.S., 2004. Concurrent EEG/fMRI analysis by multiway Partial Least Squares. NeuroImage 22, 1023–1034.
Martuzzi, R., Murray, M.M., Meuli, R.A., Thiran, J.P., Maeder, P.P., Michel, C.M., de Peralta, Grave, Menendez, R., Gonzalez Andino, S.L., 2009. Methods for determining frequency- and region-dependent relationships between estimated LFPs and BOLD responses in humans. J. Neurophysiol. 101, 491–502.
Masterton, R.A., Jackson, G.D., Abbott, D.F., 2013. Mapping brain activity using event-related independent components analysis (eICA): specific advantages for EEG–fMRI. NeuroImage 70, 164–174.
McKeown, M.J., Sejnowski, T.J., 1998. Independent component analysis of fMRI data: examining the assumptions. Hum. Brain Mapp. 6, 368–372.
Menon, V., Ford, J.M., Lim, K.O., Glover, G.H., Pfefferbaum, A., 1997. Combined event-related fMRI and EEG evidence for temporal–parietal cortex activation during target detection. Neuroreport 8, 3029–3037.
Meyer, L., Obleser, J., Kiebel, S.J., Friederici, A.D., 2012. Spatiotemporal dynamics of argument retrieval and reordering: an FMRI and EEG study on sentence processing. Front. Psychol. 3, 523.
Meyer, M.C., van Oort, E.S., Barth, M., 2013. Electrophysiological correlation patterns of resting state networks in single subjects: a combined EEG–fMRI study. Brain Topogr. 26, 98–109.
Michel, C.M., Murray, M.M., Lantz, G., Gonzalez, S., Spinelli, L., Grave de Peralta, R., 2004. EEG source imaging. Clin. Neurophysiol. 115, 2195–2222.
Mijovic, B., Vanderperren, K., Novitskiy, N., Vanrumste, B., Stiers, P., Bergh, B.V., Lagae, L., Sunaert, S., Wagemans, J., Huffel, S.V., Vos, M.D., 2012. The "why" and "how" of joint ICA: results from a visual detection task. NeuroImage 60, 1171–1185.
Mizuhara, H., Wang, L.Q., Kobayashi, K., Yamaguchi, Y., 2005. Long-range EEG phase synchronization during an arithmetic task indexes a coherent cortical network simultaneously measured by fMRI. NeuroImage 27, 553–563.
Mo, J., Liu, Y., Huang, H., Ding, M., 2013. Coupling between visual alpha oscillations and default mode activity. NeuroImage 68, 112–118.
Moosmann, M., Ritter, P., Krastel, I., Brink, A., Thees, S., Blankenburg, F., Taskin, B., Obrig, H., Villringer, A., 2003. Correlates of alpha rhythm in functional magnetic resonance imaging and near infrared spectroscopy. NeuroImage 20, 145–158.
Moosmann, M., Eichele, T., Nordby, H., Hugdahl, K., Calhoun, V.D., 2008. Joint independent component analysis for simultaneous EEG–fMRI: principle and simulation. Int. J. Psychophysiol. 67, 212–221.
Moran, R.J., Kiebel, S.J., Stephan, K.E., Reilly, R.B., Daunizeau, J., Friston, K.J., 2007. A neural mass model of spectral responses in electrophysiology. NeuroImage 37, 706–720.
Morillon, B., Lehongre, K., Frackowiak, R.S., Ducorps, A., Kleinschmidt, A., Poeppel, D., Giraud, A.L., 2010. Neurophysiological origin of human brain asymmetry for speech and language. Proc. Natl. Acad. Sci. U. S. A. 107, 18688–18693.
Mukamel, R., Gelbard, H., Arieli, A., Hasson, U., Fried, I., Malach, R., 2005. Coupling between neuronal firing, field potentials, and FMRI in human auditory cortex. Science 309, 951–954.
Mulert, C., Jager, L., Propp, S., Karch, S., Stormann, S., Pogarell, O., Moller, H.J., Juckel, G., Hegerl, U., 2005. Sound level dependence of the primary auditory cortex: simultaneous measurement with 61-channel EEG and fMRI. NeuroImage 28, 49–58.
Mulert, C., Leicht, G., Hepp, P., Kirsch, V., Karch, S., Pogarell, O., Reiser, M., Hegerl, U., Jager, L., Moller, H.J., McCarley, R.W., 2010. Single-trial coupling of the gamma-band response and the corresponding BOLD signal. NeuroImage 49, 2238–2247.
Mullinger, K., Bowtell, R., 2011. Combining EEG and fMRI. Methods Mol. Biol. 711, 303–326.
Mullinger, K., Brookes, M., Stevenson, C., Morgan, P., Bowtell, R., 2008a. Exploring the feasibility of simultaneous electroencephalography/functional magnetic resonance imaging at 7 T. Magn. Reson. Imaging 26, 968–977.
Mullinger, K., Debener, S., Coxon, R., Bowtell, R., 2008b. Effects of simultaneous EEG recording on MRI data quality at 1.5, 3 and 7 Tesla. Int. J. Psychophysiol. 67, 178–188.
Mullinger, K.J., Havenhand, J., Bowtell, R., 2013. Identifying the sources of the pulse artefact in EEG recordings made inside an MR scanner. NeuroImage 71, 75–83.
Murta, T., Leal, A., Garrido, M.I., Figueiredo, P., 2012. Dynamic Causal Modelling of epileptic seizure propagation pathways: a combined EEG–fMRI study. NeuroImage 62, 1634–1642.
Nagai, Y., Critchley, H.D., Featherstone, E., Fenwick, P.B., Trimble, M.R., Dolan, R.J., 2004. Brain activity relating to the contingent negative variation: an fMRI investigation. NeuroImage 21, 1232–1241.
Niazy, R.K., Beckmann, C.F., Iannetti, G.D., Brady, J.M., Smith, S.M., 2005. Removal of FMRI environment artifacts from EEG data using optimal basis sets. NeuroImage 28, 720–737.
Niedermeyer, E., Lopes da Silva, F.H., 2005. Electroencephalography: Basic Principles, Clinical Applications, and Related Fields, 5th ed. Lippincott Williams & Wilkins, Philadelphia.
Nierhaus, T., Gundlach, C., Goltz, D., Thiel, S.D., Pleger, B., Villringer, A., 2013. Internal ventilation system of MR scanners induces specific EEG artifact during simultaneous EEG–fMRI. NeuroImage 74, 70–76.

Niessing, J., Ebisch, B., Schmidt, K.E., Niessing, M., Singer, W., Galuske, R.A., 2005. Hemodynamic signals correlate tightly with synchronized gamma oscillations. Science 309, 948–951.
Novitski, N., Anourova, I., Martinkauppi, S., Aronen, H.J., Naatanen, R., Carlson, S., 2003. Effects of noise from functional magnetic resonance imaging on auditory event-related potentials in working memory task. NeuroImage 20, 1320–1328.
Novitskiy, N., Ramautar, J.R., Vanderperren, K., De Vos, M., Mennes, M., Mijovic, B., Vanrumste, B., Stiers, P., Van den Bergh, B., Lagae, L., Sunaert, S., Van Huffel, S., Wagemans, J., 2011. The BOLD correlates of the visual P1 and N1 in single-trial analysis of simultaneous EEG–fMRI recordings during a spatial detection task. NeuroImage 54, 824–835.
Nunez, P.L., Silberstein, R.B., 2000. On the relationship of synaptic activity to macroscopic measurements: does co-registration of EEG with fMRI make sense? Brain Topogr. 13, 79–96.
Ogawa, S., Lee, T.M., Kay, A.R., Tank, D.W., 1990. Brain magnetic resonance imaging with contrast dependent on blood oxygenation. Proc. Natl. Acad. Sci. U. S. A. 87, 9868–9872.
Ostwald, D., Porcaro, C., Bagshaw, A.P., 2010. An information theoretic approach to EEG–fMRI integration of visually evoked responses. NeuroImage 49, 498–516.
Ostwald, D., Porcaro, C., Bagshaw, A.P., 2011. Voxel-wise information theoretic EEG–fMRI feature integration. NeuroImage 55, 1270–1286.
Ou, W., Nummenmaa, A., Ahveninen, J., Belliveau, J.W., Hamalainen, M.S., Golland, P., 2010. Multimodal functional imaging using fMRI-informed regional EEG/MEG source estimation. NeuroImage 52, 97–108.
Patel, M.R., Blum, A., Pearlman, J.D., Yousuf, N., Ives, J.R., Saeteng, S., Schomer, D.L., Edelman, R.R., 1999. Echo-planar functional MR imaging of epilepsy with concurrent EEG monitoring. AJNR Am. J. Neuroradiol. 20, 1916–1919.
Pfurtscheller, G., Lopes da Silva, F.H., 1999. Event-related EEG/MEG synchronization and desynchronization: basic principles. Clin. Neurophysiol. 110, 1842–1857.
Philiastides, M.G., Sajda, P., 2006. Temporal characterization of the neural correlates of perceptual decision making in the human brain. Cereb. Cortex 16, 509–518.
Philiastides, M.G., Sajda, P., 2007. EEG-informed fMRI reveals spatiotemporal characteristics of perceptual decision making. J. Neurosci. 27, 13082–13091.
Raichle, M.E., Gusnard, D.A., 2005. Intrinsic brain activity sets the stage for expression of motivated behavior. J. Comp. Neurol. 493, 167–176.
Rauch, A., Rainer, G., Logothetis, N.K., 2008. The effect of a serotonin-induced dissociation between spiking and perisynaptic activity on BOLD functional MRI. Proc. Natl. Acad. Sci. U. S. A. 105, 6759–6764.
Regenbogen, C., De Vos, M., Debener, S., Turetsky, B.I., Mossnang, C., Finkelmeyer, A., Habel, U., Neuner, I., Kellermann, T., 2012. Auditory processing under cross-modal visual load investigated with simultaneous EEG–fMRI. PLoS One 7, e52267.
Riera, J.J., Sumiyoshi, A., 2010. Brain oscillations: ideal scenery to understand the neurovascular coupling. Curr. Opin. Neurol. 23, 374–381.
Riera, J.J., Wan, X., Jimenez, J.C., Kawashima, R., 2006. Nonlinear local electrovascular coupling. I: a theoretical model. Hum. Brain Mapp. 27, 896–914.
Riera, J.J., Jimenez, J.C., Wan, X., Kawashima, R., Ozaki, T., 2007. Nonlinear local electrovascular coupling. II: from data to neuronal masses. Hum. Brain Mapp. 28, 335–354.
Rosa, M.J., Daunizeau, J., Friston, K.J., 2010a. EEG–fMRI integration: a critical review of biophysical modeling and data analysis approaches. J. Integr. Neurosci. 9, 453–476.
Rosa, M.J., Kilner, J., Blankenburg, F., Josephs, O., Penny, W., 2010b. Estimating the transfer function from neuronal activity to BOLD using simultaneous EEG–fMRI. NeuroImage 49, 1496–1509.
Rosa, M.J., Kilner, J.M., Penny, W.D., 2011. Bayesian comparison of neurovascular coupling models using EEG–fMRI. PLoS Comput. Biol. 7, e1002070.
Sammer, G., Blecker, C., Gebhardt, H., Kirsch, P., Stark, R., Vaitl, D., 2005. Acquisition of typical EEG waveforms during fMRI: SSVEP, LRP, and frontal theta. NeuroImage 24, 1012–1024.
Scheeringa, R., Bastiaansen, M.C., Petersson, K.M., Oostenveld, R., Norris, D.G., Hagoort, P., 2008. Frontal theta EEG activity correlates negatively with the default mode network in resting state. Int. J. Psychophysiol. 67, 242–251.
Scheeringa, R., Fries, P., Petersson, K.M., Oostenveld, R., Grothe, I., Norris, D.G., Hagoort, P., Bastiaansen, M.C., 2011. Neuronal dynamics underlying high- and low-frequency EEG oscillations contribute independently to the human BOLD signal. Neuron 69, 572–583.
Schicke, T., Muckli, L., Beer, A.L., Wibral, M., Singer, W., Goebel, R., Rosler, F., Roder, B., 2006. Tight covariation of BOLD signal changes and slow ERPs in the parietal cortex in a parametric spatial imagery task with haptic acquisition. Eur. J. Neurosci. 23, 1910–1918.
Scholvinck, M.L., Maier, A., Ye, F.Q., Duyn, J.H., Leopold, D.A., 2010. Neural basis of global resting-state fMRI activity. Proc. Natl. Acad. Sci. U. S. A. 107, 10238–10243.
Schummers, J., Yu, H., Sur, M., 2008. Tuned responses of astrocytes and their influence on hemodynamic signals in the visual cortex. Science 320, 1638–1643.
Shmuel, A., Augath, M., Oeltermann, A., Logothetis, N.K., 2006. Negative functional MRI response correlates with decreases in neuronal activity in monkey visual area V1. Nat. Neurosci. 9, 569–577.
Singh, M., Kim, S., Kim, T.S., 2003. Correlation between BOLD–fMRI and EEG signal changes in response to visual stimulus frequency in humans. Magn. Reson. Med. 49, 108–114.
Smith, S.M., Jenkinson, M., Woolrich, M.W., Beckmann, C.F., Behrens, T.E., Johansen-Berg, H., Bannister, P.R., De Luca, M., Drobnjak, I., Flitney, D.E., Niazy, R.K., Saunders, J., Vickers, J., Zhang, Y., De Stefano, N., Brady, J.M., Matthews, P.M., 2004. Advances in functional and structural MR image analysis and implementation as FSL. NeuroImage 23 (Suppl. 1), S208–S219.
Sotero, R.C., Trujillo-Barreto, N.J., 2007. Modelling the role of excitatory and inhibitory neuronal activity in the generation of the BOLD signal. NeuroImage 35, 149–165.
Sotero, R.C., Trujillo-Barreto, N.J., 2008. Biophysical model for integrating neuronal activity, EEG, fMRI and metabolism. NeuroImage 39, 290–309.
Strother, S.C., 2006. Evaluating fMRI preprocessing pipelines. IEEE Eng. Med. Biol. Mag. 25, 27–41.
Tallon-Baudry, C., Bertrand, O., Peronnet, F., Pernier, J., 1998. Induced gamma-band activity during the delay of a visual short-term memory task in humans. J. Neurosci. 18, 4244–4254.
Thomson, D.J., 1982. Spectrum estimation and harmonic-analysis. Proc. IEEE 70, 1055–1096.
Thornton, R.C., Rodionov, R., Laufs, H., Vulliemoz, S., Vaudano, A., Carmichael, D., Cannadathu, S., Guye, M., McEvoy, A., Lhatoo, S., Bartolomei, F., Chauvel, P., Diehl, B., De Martino, F., Elwes, R.D., Walker, M.C., Duncan, J.S., Lemieux, L., 2010. Imaging haemodynamic changes related to seizures: comparison of EEG-based general linear model, independent component analysis of fMRI and intracranial EEG. NeuroImage 53, 196–205.
Tyvaert, L., Hawco, C., Kobayashi, E., LeVan, P., Dubeau, F., Gotman, J., 2008. Different structures involved during ictal and interictal epileptic activity in malformations of cortical development: an EEG–fMRI study. Brain 131, 2042–2060.
Ullsperger, M., von Cramon, D.Y., 2001. Subprocesses of performance monitoring: a dissociation of error processing and response competition revealed by event-related fMRI and ERPs. NeuroImage 14, 1387–1401.
Valdes-Sosa, P.A., Sanchez-Bornot, J.M., Sotero, R.C., Iturria-Medina, Y., Aleman-Gomez, Y., Bosch-Bayard, J., Carbonell, F., Ozaki, T., 2009. Model driven EEG/fMRI fusion of brain oscillations. Hum. Brain Mapp. 30, 2701–2721.
Vanni, S., Warnking, J., Dojat, M., Delon-Martin, C., Bullier, J., Segebarth, C., 2004. Sequence of pattern onset responses in the human visual areas: an fMRI constrained VEP source analysis. NeuroImage 21, 801–817.
Vasios, C.E., Angelone, L.M., Purdon, P.L., Ahveninen, J., Belliveau, J.W., Bonmassar, G., 2006. EEG/(f)MRI measurements at 7 Tesla using a new EEG cap ("InkCap"). NeuroImage 33, 1082–1092.
Vulliemoz, S., Rodionov, R., Carmichael, D.W., Thornton, R., Guye, M., Lhatoo, S.D., Michel, C.M., Duncan, J.S., Lemieux, L., 2010. Continuous EEG source imaging enhances analysis of EEG–fMRI in focal epilepsy. NeuroImage 49, 3219–3229.
Vulliemoz, S., Carmichael, D.W., Rosenkranz, K., Diehl, B., Rodionov, R., Walker, M.C., McEvoy, A.W., Lemieux, L., 2011. Simultaneous intracranial EEG and fMRI of interictal epileptic discharges in humans. NeuroImage 54, 182–190.
Wan, X., Riera, J., Iwata, K., Takahashi, M., Wakabayashi, T., Kawashima, R., 2006. The neural basis of the hemodynamic response nonlinearity in human primary visual cortex: implications for neurovascular coupling mechanism. NeuroImage 32, 616–625.
Whitman, J.C., Ward, L.M., Woodward, T.S., 2013. Patterns of cortical oscillations organize neural activity into whole-brain functional networks evident in the fMRI BOLD signal. Front. Hum. Neurosci. 7, 80.
Whittingstall, K., Logothetis, N.K., 2009. Frequency–band coupling in surface EEG reflects spiking activity in monkey visual cortex. Neuron 64, 281–289.
Wolters, C.H., Anwander, A., Tricoche, X., Weinstein, D., Koch, M.A., MacLeod, R.S., 2006. Influence of tissue conductivity anisotropy on EEG/MEG field and return current computation in a realistic head model: a simulation and visualization study using high-resolution finite element modeling. NeuroImage 30, 813–826.
Worsley, K.J., Friston, K.J., 1995. Analysis of fMRI time-series revisited—again. NeuroImage 2, 173–181.
Yacoub, E., Shmuel, A., Logothetis, N., Ugurbil, K., 2007. Robust detection of ocular dominance columns in humans using Hahn Spin Echo BOLD functional MRI at 7 Tesla. NeuroImage 37, 1161–1177.
Yang, L., Liu, Z., He, B., 2010. EEG–fMRI reciprocal functional neuroimaging. Clin. Neurophysiol. 121, 1240–1250.
Yuan, H., Liu, T., Szarkowski, R., Rios, C., Ashe, J., He, B., 2010. Negative covariation between task-related responses in alpha/beta-band activity and BOLD in human sensorimotor cortex: an EEG and fMRI study of motor imagery and movements. NeuroImage 49, 2596–2606.
Yuan, H., Zotev, V., Phillips, R., Drevets, W.C., Bodurka, J., 2012. Spatiotemporal dynamics of the brain at rest—exploring EEG microstates as electrophysiological signatures of BOLD resting state networks. NeuroImage 60, 2062–2072.
Zheng, Y., Martindale, J., Johnston, D., Jones, M., Berwick, J., Mayhew, J., 2002. A model of the hemodynamic response and oxygen delivery to brain. NeuroImage 16, 617–637.